DATA-DRIVEN MODELING OF BOREHOLE THERMAL ENERGY STORAGE (BTES) FOR OPERATIONAL OPTIMIZATION OF RENEWABLE HEAT PRODUCTION SYSTEMS

Hannes Gernandt[1,2], Willem Hagemann[1]*, Franziska Krenzlin[1], Johannes Schiffer[1,3]

[1] Fraunhofer Einrichtung für Energieinfrastrukturen und Geothermie IEG, Gulbener Straße 23, 03046 Cottbus, Germany

[2] IMACM, Bergische Universität Wuppertal, Gaußstraße 20, 42119 Wuppertal, Germany

[3] FG Regelungs- und Netzleittechnik, Brandenburgische Technische Universität Cottbus-Senftenberg, Siemens-Halske-Ring 14, 03046 Cottbus, Germany

*Corresponding Author: willem.hagemann@ieg.fraunhofer.de

ABSTRACT

The utilization of underground thermal energy storage (UTES) systems, such as borehole thermal energy storage (BTES) systems plays a crucial role in the decarbonization of district heating. To ensure high performance and operation efficiency under the condition of a robust system operation, heat supply systems require advanced control and operation strategies including the operation of the thermal storage systems. The focus of our operational optimization lies on the heat production side, comprising a BTES and diverse heat sources, buffer storage systems and heat pumps. We utilize a nonlinear model of the heating network that explicitly integrates mass flows and temperatures instead of solely relying on heat flow considerations. The advantage of this more detailed consideration is that realistic constraints on temperatures and mass flows can be easily incorporated into the model. A major challenge in such realistic modeling is the correct representation of the temperature dynamics of thermal storage components, especially when the storage parameters are unknown and only limited input-output data are available. In this work, we propose a novel method leading to a reduced surrogate model of the BTES temperature dynamics that can be directly included in the optimization or control algorithms. The resulting data-based surrogate model captures the fundamental dynamics while being deployable to operational optimization and system control algorithms. In particular, we employ a Python-based operational optimization process of a theoretical system setup using Pyomo. In conclusion, the presented storage modeling approach is a first step towards a broad variety of system configurations including different UTES types.

1 INTRODUCTION

The EU's climate strategy aims for complete net decarbonization by 2050 (European Union, 2020). A key element in this context is the decarbonization of the heating sector, which is currently largely based on fossil energy generation (77.1%) (Eurostat, 2022). In a decarbonized energy system, various volatile generation technologies (industrial waste heat, solar thermal energy) are coupled with consumers (district heating consumers) via short- and long-term storage devices, with sector coupling taking place via the use of heat pumps. In such an integrated energy system, the optimization of coupled system operation can make an important contribution to the efficient use of resources by reducing peak energy generation and maximizing the exploitation of available renewable energy potentials.

Seasonal thermal energy storage systems are a central component for implementing the transformation to renewable heat generation by counteracting the mismatch between renewable energy potentials and heat demand as shown by Victoria *et al.* (2019) and Abdur Rehman *et al.* (2021).

https://doi.org/10.52202/077185-0157

In this paper, we focus on the thermal management of several heat sources on the production side, such as waste and solar thermal heat, which are, in combination with geothermal storage systems the most common renewable heat sources. A schematic of the system setup is presented in Figure 1. The goal of the control strategy is to match a given heat demand by adjusting the mass flows and to operate the Power-to-Heat units, e.g., such that the operational costs are minimized. We will refer to this methodology as *energy operational optimization*. Here, we consider a heat pump and an electric heater, whose electricity consumption is minimized, leading to the minimization of the deployment of rare and expensive peak load energy.

In this paper, we formulate a model for the heat production system that integrates mass flows and temperatures. In contrast to operational optimization models solely reliant on heat flow considerations, our approach furnishes a more precise representation of the actual behavior of the system.

The most challenging part is to accurately model the UTES. In the context of simulations, the use of finite-element models (FEMs) is quite popular and there are several simulation software packages available, such as Feflow or Spring. Although these software packages provide accurate models for simulation, such packages typically do not include optimization frameworks and therefore the combination with another software is needed to perform the operational optimization. Hence, the second significant contribution lies in introducing a novel method for constructing a reduced-order surrogate data-based models for BTES, effectively encapsulating their temperature dynamics. This model is based on a parametrized BTES model from Fiorentini *et al.* (2023), whose system coefficients are assumed to depend explicitly on the mass flow rates. The unknown system parameters are then recovered from the simulation data that are obtained for fixed mass-flow rates. For fixed mass flow rates, we derive linear system dynamics, enabling the application of a conventional system identification technique known as the Kalman-Ho algorithm or the eigensystem realization algorithm, see e.g. De Schutter (2000). The resulting identified data-based surrogate model can be directly integrated into an optimization framework, such as the Python toolbox Pyomo, see Bynum *et al.* (2021) and Hart *et al.* (2011).

The concept of developing surrogate models for UTES is not novel. A comparable methodology was previously employed in a study by Fiorentini *et al.* (2023) for design optimization of a BTES within a heating network. Other approaches that include simplified models of UTES in the context of optimizing the system operation have been used in Fiorentini and Baldini (2021) and Saloux and Candanedo (2019), where an RC-type model was developed, and in Gabrieli et al. (2020), where the g-function was utilized. Furthermore, reduced order models of borehole heat exchangers were derived in Verhelst and Helsen (2011). Although these models can provide accurate models for the temperature dynamics, this often requires a time-demanding adaptation of a large number of model parameters accounting for site-specific geological conditions and might also involve restrictive assumptions on the geometry of the BTES. In our methodology, we streamline the process by generating the surrogate model in a single step. This is achieved by applying our algorithm directly to simulation data, resulting in the creation of data-based surrogate models. These models can subsequently be seamlessly integrated as constraints in the energy operational optimization problem.

Summarizing, the main contributions of this paper are the following:

1. we derive a mass-flow and temperature-based model of the multiple-sources heat production system;
2. we provide a method for constructing a reduced order surrogate model of a BTES based on simulation data;
3. we integrate our BTES model in a Python-based energy operational optimization of the overall multiple-sources heat production system using Pyomo.

The article is structured as follows: Section 2 describes the topology of the heating network and the components considered. Section 3 explains our approach for creating black-box models from input-output data. This method is used in Section 4 to derive the data-based surrogate model. Section 5 demonstrates the method using an example system comprising a BTES on the heat generator side

https://doi.org/10.52202/077185-0157

connected to the heat demand side via a heat pump. First, we derive a data-based surrogate model for the BTES and then integrate it as a constraint in the optimization problem, which aims to minimize the total annual electricity consumption.

2 MODELING OF MULTIPLE SOURCES HEATING NETWORKS

The overall heating network can be viewed as a graph, whose edges model the transmission pipes or heat sources allowing for heat exchange and whose vertices represent either pipe junctions or heat storage systems as Figure 1 illustrates graphically. The heat exchange is established via the edges, where each edge has a mass flow $\dot{m} \geq 0$, as well as ingoing and outgoing temperatures T_{in} and T_{out}, respectively. Hence, the heat flow $\dot{Q}$ that is exchanged via the considered edge is given by

$$\dot{Q} = c_p \cdot \dot{m} \cdot \Delta T, \qquad \Delta T = T_{out} - T_{in}, \tag{1}$$

where $c_p = 4182\, J(kg \cdot K)^{-1}$ is the specific heat of water. To allow for optimal operation and control of the thermal system, we need to consider dynamic models for the change of temperature in each of the multiple heat sources. The interconnection of some exemplary heat sources is shown in Figure 1. Note that while this sketch and the following network description serve as a blueprint for the integration of several underground storage systems, in this article we consider the specific integration of a BTES.

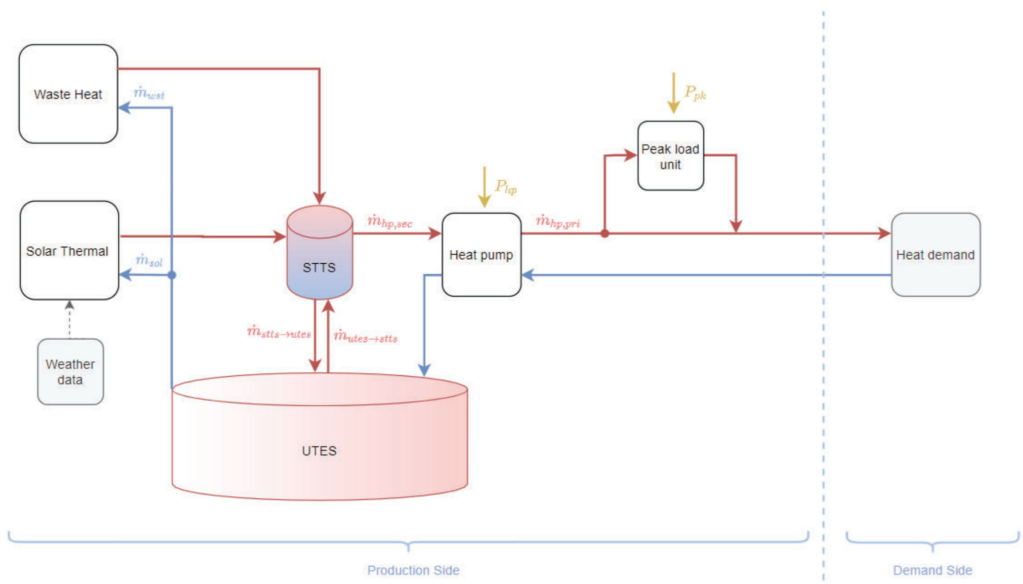

Figure 1: Schematic of the considered heating network including the mass flows $\dot{m}$ between the units and the electrical power P_{hp} and P_{pk} used by the heat pump and the peak unit. STTS denotes a short-term thermal energy storage.

The system operation on the production side can be described as follows: The water stored in the UTES with temperature T_{utes} is pumped via mass flows $\dot{m}_{sol}$ and $\dot{m}_{wst}$ towards the solar thermal and the waste heat source, respectively. The heated water then enters the short-term buffer storage STTS. The mass flow exiting the STTS is then split up into $\dot{m}_{stts\to utes}$ and $\dot{m}_{hp,sec}$ where $\dot{m}_{stts\to utes}$ is directly pumped into the UTES and $\dot{m}_{hp,sec}$ is used as a heating source for the heat pump. Besides this, there is an additional feed $\dot{m}_{utes\to stts}$ to the buffer storage from the UTES.

https://doi.org/10.52202/077185-0157

On the production side, we consider waste heat and solar thermal heat sources. We assume that there is an internal controller at both components that regulates the output temperature, such that a given constant temperature increase ΔT is achieved. This means that according to (1) the solar thermal power and the waste heat power at time instance $k \geq 0$ satisfy

$$\dot{Q}_{sol}(k) = c_p \cdot \dot{m}_{sol}(k) \cdot \Delta T_{sol} \quad \text{and} \quad \dot{Q}_{wst}(k) = c_p \cdot \dot{m}_{wst}(k) \cdot \Delta T_{wst}. \tag{2}$$

Consequently, if the produced heat powers $\dot{Q}_{sol}(k)$ and $\dot{Q}_{wst}(k)$ are known, we can determine the mass flows $\dot{m}_{sol}(k)$ and $\dot{m}_{wst}(k)$ from (2).

On the demand side, the model includes a peak load unit and the heat demand. The heat demand is modeled as a sequence of hourly requested heat flows, organized into variable supply and return temperatures and mass flows, which are based on the demand curves of a realistic district heating network. A heat pump is placed between the production side and the demand side. The heat pump is described by the following set of equations, see Petrecca (1993)

$$\dot{Q}_{hp,pri}(k) = COP(k) \cdot P_{hp}(k) = \dot{Q}_{hp,sec}(k) + P_{hp}(k), \tag{3}$$

$$\dot{Q}_{hp,sec}(k) = c_p \cdot \dot{m}_{hp,sec}(k) \cdot \Delta T_{hp,\,sec}(k),\ \dot{Q}_{hp,pri}(k) = c_p \cdot \dot{m}_{hp,pri}(k) \cdot \Delta T_{hp,\,pri}(k), \tag{4}$$

$$COP(k)_{Carnot} = \frac{T_{hp,pri}(k)}{T_{hp,pri}(k) - T_{hp,sec}(k)} \quad \text{and} \quad COP(k) = \eta \cdot \frac{T_{hp,pri}(k)}{T_{hp,pri}(k) - T_{hp,sec}(k)}, \tag{5}$$

where COP_{Carnot} represents the theoretical maximum coefficient of performance. Losses that occur in reality are summarized in the grade of quality η, for which we assume $\eta = 0.5$ according to Arpagaus *et al.* (2018). The actual COP is calculated as the product of the COP_{Carnot} and η. Furthermore, P_{hp} is the electric power consumed by the heat pump, $T_{hp,sec}$ is the fluid temperature on the secondary side of the heat pump, and $T_{hp,pri}$ is the temperature on the primary side. $T_{hp,pri}$ is bounded by the return temperature and supply temperature of the heat demand. There is an additional electric heater on the demand side to cover potential peak demands that can be described by

$$\dot{Q}_{pk}(k) = \eta_{pk} P_{pk}(k), \qquad k = 0,1, \ldots, \tag{6}$$

where $\dot{Q}_{pk}$ is the produced heat flow, $\eta_{pk} = 1.0$ (Münnich *et al.*, 2022) is the assumed efficiency of the heater and P_{pk} is the consumed electrical power.

On the primary side, we assume a given heat demand $\dot{Q}_{dem}$, which must be met by the heat generated by the peak load unit and the heat pump, i.e.,

$$\dot{Q}_{dem}(k) = \eta_{pk} P_{pk}(k) + COP(k) P_{hp}(k), \qquad k \geq 0. \tag{7}$$

Furthermore, the considered heating network has two storage units: an underground thermal energy storage (UTES), as well as a buffer storage (STTS) between the multiple heat sources and the secondary side of the heat pump. The time evolution of the water temperature T_{stts} in the buffer storage is based on Machado *et al.* (2022) and can be described by

$$T_{stts}(k+1) = T_{stts}(k) + \frac{\Delta t}{c_p \rho_w V_{stts}} \left(\dot{Q}_{in}(k) - \dot{Q}_{out}(k) \right) - l_{stts}(T_{stts}(k) - T_a), k \geq 0, \tag{8}$$

where ρ_w is the density of water in $kg \cdot m^{-3}$, V_{tes} is the storage volume in m^3, Δt is the discretization step size in seconds s, l_{stts} is a parameter that characterizes the heat loss relative to the ambient temperature T_a, and $\dot{Q}_{in}$ and $\dot{Q}_{out}$ are the thermal input and output powers in Watt W, respectively. The parameter l_{stts} was selected such that it corresponds to a heat loss of 1.7% per week, see Danish Energy Agency (2023). To maintain the constant storage volume V_{stts} in (8), we require the following balance of mass flow rates to hold:

https://doi.org/10.52202/077185-0157

$$\dot m_{sol}(k) + \dot m_{wst}(k) + \dot m_{utes\to stts}(k) = \dot m_{stts\to utes}(k) + \dot m_{hp,sec}. \tag{9}$$

Next, replacing the thermal power using (1) results in

$$\begin{aligned} {c_p}^{-1}\dot Q_{in}(k) &= \dot m_{sol}(k)\,(T_{utes}(k) + \Delta T_{sol}) + \dot m_{wst}(k)\,(T_{utes}(k) + \Delta T_{wst}) \\ &\quad + \dot m_{utes\to stts}(k)\,T_{utes}(k), \\ {c_p}^{-1}\dot Q_{out}(k) &= \dot m_{hp,sec}(k)\,T_{stts}(k) + \dot m_{stts\to utes}(k)\,T_{stts}(k). \end{aligned} \tag{10}$$

Note, that after this replacement of $\dot Q_{in}$ and $\dot Q_{out}$ it becomes obvious that (8) models a nonlinear dynamic relationship between the storage temperature and the incoming mass flows and their temperatures.

For the UTEs, we analogously begin with a linear dynamic relationship of the storage temperature and the incoming and outgoing heat flows and obtain the full nonlinear dynamics after factoring the heat flows into their corresponding mass flows and temperatures. Based on the STTS model (8), we will use the following dynamic black-box model that will be obtained from data, cf. Section 3,

$$\begin{aligned} x(k+1) &= Ax(k) + Bu(k) + d(k),\ \ k \ge 0, \qquad x(0) = x_0, \\ y(k) &= Cx(k) + Du(k), \end{aligned} \tag{11}$$

where $A \in \mathbb{R}^{n\times n}$, $B \in \mathbb{R}^{n\times m}$, $C \in \mathbb{R}^{l\times n}$, and $D \in \mathbb{R}^{l\times m}$ are unknown system matrices, $x(k) \in \mathbb{R}^n$ is an unknown system state, $y(k) \in \mathbb{R}^l$ is the output, $u(k) \in \mathbb{R}^m$ is the control input, and $d(k) \in \mathbb{R}^n$ is an unknown disturbance, which models e.g. the influence of the ambient temperature. Since we construct the black-box model from input-output data generated by a simulation model of the UTES, we can choose the inputs and outputs to be

$$u(k) = c_p \cdot \dot m_{utes,in}(k) \cdot T_{utes,in}(k) \quad \text{and} \quad y(k) = c_p \cdot \dot m_{utes,out}(k) \cdot T_{utes}(k), \tag{12}$$

where $\dot m_{utes,out}(k)$ and $\dot m_{utes,in}(k)$ are the mass flows leaving and entering the UTES, respectively, and $T_{utes,in}(k)$ is the input temperature into the UTES that is given by the perfect mixing model

$$T_{utes,in}(k) = \frac{\dot m_{stts\to utes}(k)T_{stts}(k) \ + \ \dot m_{hp,sec}(k)\,(T_{stts}(k) \ + \ \Delta T_{hp})}{\dot m_{wst}(k) \ + \ \dot m_{utes\to stts}(k) \ + \ \dot m_{sol}(k)}. \tag{13}$$

3 CONTROL-ORIENTED BLACK-BOX MODELS FOR SYSTEM COMPONENTS

In this section, we describe a general approach to obtain control-oriented black-box models based on simulation data. This approach will be applied in Section 4 to simulation data from a BTES system to derive our data-based surrogate model. By a control-oriented model we mean a linear time-invariant system with matrix coefficients (A, B, C, D) of the form (11).

We describe a method for obtaining the unknown matrices (A, B, C, D) in (11) that fit to the simulated system input-output data $\{(u(k), y(k))\}_{k\ge 0}$.

First, note that the solution of (11) is given by

$$x(k) = A^k x_0 + \textstyle\sum_{j=0}^{k-1} A^{k-j-1}\big(Bu(j) + d(j)\big), \tag{14}$$

from which the output $y(k)$ can be easily obtained using the last equation in (11). Hence, if we consider two sets of simulation data $\{(u_1(k), y_1(k))\}_{k\ge 0}$ and $\{(u_2(k), y_2(k))\}_{k\ge 0}$ that were obtained using the same initial value x_0 and disturbance values d, then taking the difference of the solutions results in

https://doi.org/10.52202/077185-0157

$$x_2(k) - x_1(k) = \sum_{j=0}^{k-1} A^{k-j-1} B\big(u_2(j) - u_1(j)\big), \tag{15}$$

which does neither depend on the initial value x_0 nor the disturbance variables d. Therefore, it is sufficient to focus on the case $x_0 = 0$ and $d = 0$. For simplicity, we restrict ourselves to the one-dimensional case $u(k), y(k) \in \mathbb{R}$, i.e. $m = l = 1$. Note, however, that the following construction can be easily extended to arbitrary dimensions of the inputs and outputs vectors, i.e. $l, m \geq 1$, by considering the entries of the input and output vectors separately.

After choosing the input as $u(0) = 1,\ u(k) = 0,\ k \geq 1$, we obtain the following

$$\begin{aligned} D &= Cx(0) + Du(0) = y(0), \\ B &= Ax(0) + Bu(0) = x(1), \\ CB &= Cx(1) + Du(1) = y(1). \end{aligned} \tag{16}$$

More generally, this leads to

$$y(k+1) = Cx(k+1) + Du(k+1) = C\big(Ax(k) + Bu(k)\big) + Du(k) = CA^{k-1}B, \quad k \geq 0 \tag{17}$$

which defines the so-called Markov parameters of the system. The black-box model (A, B, C, D) can be recovered using the Hankel matrix and the shifted Hankel matrix, i.e.,

$$\begin{aligned} H_{r,r'} &= \begin{pmatrix} y(1) & y(2) & y(3) & \dots & y(r') \\ y(2) & y(3) & y(4) & \dots & y(r'+1) \\ \vdots & \vdots & \vdots & & \vdots \\ y(r) & y(r+1) & y(r+2) & \dots & y(r'+r-1) \end{pmatrix}, \\ \overline{H}_{r,r'} &= \begin{pmatrix} y(2) & y(3) & y(4) & \dots & y(r'+1) \\ y(3) & y(4) & y(5) & \dots & y(r'+2) \\ \vdots & \vdots & \vdots & & \vdots \\ y(r+1) & y(r+2) & y(r+3) & \dots & y(r'+r) \end{pmatrix}. \end{aligned} \tag{18}$$

In the following we state the Kalman-Ho algorithm, see e.g. Section 3.3 in De Schutter (2000) that allows us to recover the matrices (A, B, C, D) by performing the following steps:

1. Select r large enough and determine $\rho = \operatorname{rank}\big(H_{r,r}\big)$.
2. Find nonsingular $U, V \in \mathbb{R}^{n\times n}$, such that the following holds

   $$UH_{r,r}V = \begin{pmatrix} I_\rho & 0 \\ 0 & 0 \end{pmatrix}, \tag{19}$$

   where $I_\rho \in \mathbb{R}^{\rho\times\rho}$ is the identity matrix.
3. Using $E_{p,q} = (I_p \quad 0_{p,q-p})$ define the system matrices as follows:

   $$A = E_{\rho,r} P \overline{H}_{r,r} Q E_{\rho,r}^\top, \qquad B = E_{\rho,r} P H_{r,r} E_{1,r}^\top, \qquad C = E_{1,r} H_{r,r} Q E_{\rho,r}^\top, \qquad D = y(0). \tag{20}$$

Note that we consider the rank of the matrix in step 1, i.e. the number of linearly independent rows (and columns). A standard method to achieve the decomposition in step 2 is the singular value decomposition for which the matrices $U, V \in \mathbb{R}^{n\times n}$ are orthogonal, i.e. $U \cdot U^\top = V \cdot V^\top = I_n$ holds.

https://doi.org/10.52202/077185-0157

4 DERIVATION OF A DATA-BASED SURROGATE BTES MODEL

In this section we derive a data-based model for given input-output data of a BTES. To this end we start with a simplified BTES model with linear temperature dynamics from Fiorentini *et al.* (2023) of the following form

$$T_{BT}(k+1) = T_{BT}(k) + \frac{\Delta t}{\rho_g c_{p,g} V}\left(\dot{Q}_{grid}(k) - UA\big(T_{BT}(k) - T_a(k)\big) - k_g h \frac{D}{2}\big(T_{BT}(k) - T_g\big)\right) \quad (21)$$

with the averaged BTES temperature T_{BT}, density of the ground ρ_g, the specific heat of the ground $c_{p,g}$, the BTES volume V, the BTES depth D, the UA value, the thermal conductivity of the ground k_g, the ambient temperature $T_a(k)$, the temperature of the ground T_g, the discretization step size Δt, and the heat flow $\dot{Q}_{grid}(k)$ that is exchanged with the primary side.

The input of this model is the heat flow into the storage and the output is considered to be $y(k) = T_{BT}(k)$. We assume that the parameter values of the system dynamics are unknown and the aim is to determine these parameters from the input-output data using the method described in Section 3. To this end, the terms are resorted to obtain a linear system

$$T_{BT}(k+1) = A\, T_{BT}(k) + B\, \dot{Q}_{grid}(k) + d(k) \quad (22)$$

with

$$A = 1 - \frac{\Delta t}{\rho_g c_{p,g} V}\left(UA + k_g h \frac{D}{2}\right), \qquad B = \frac{\Delta t}{\rho_g c_{p,g} V}, \;\; d(k) = \frac{\Delta t}{\rho_g c_{p,g} V}\left(k_g h \frac{D}{2} T_g + UA T_a(k)\right) \quad (23)$$

Next, the heat flow that is exchanged with the network is replaced using the expression (1) which includes the input mass flow and the temperatures

$$\dot{Q}_{grid}(k) = c_p\big(T_{in}(k) - T_{BT}(k)\big)\dot{m}_{utes,in}(k), \qquad \dot{m}_{utes,in}(k) = \dot{m}_{utes,out}(k). \quad (24)$$

However, this results in a nonlinear system model, or more precisely, a linear parameter varying model,

$$A\big(\dot{m}(k)\big) = A - c_p \cdot B \cdot \dot{m}(k), \qquad B\big(\dot{m}(k)\big) = c_p \cdot B \cdot \dot{m}(k), \quad (25)$$

such that the identification method from Section 3 cannot be applied directly. In fact, the yet unknown parameters in (21) can be identified by restricting the mass flows to be constant, i.e. $\dot{m}_{utes,in}(k) = \dot{m}_{fix}$ and by considering only the input temperature $u(k) = T_{in}(k)$ as a control input. This results in a linear system, to which the identification method from Section 3 can be applied to determine the coefficients A and B in (22). Subsequently, by replacing $\dot{Q}_{grid}(k)$ in equation (22) with (24), we obtain a BTES model with time-varying mass flows that can then be used as optimization variables in the operational optimization of the system shown in Figure 1.

To determine the unknown coefficients A and B in (22), we generate two sets of simulation data $\{\big(u_1(k), y_1(k)\big)\}_{k\geq 0}$ and $\{\big(u_2(k), y_2(k)\big)\}_{k\geq 0}$ for the considered fixed mass flow and for two choices of input temperature sequences $u_1(k) = (T_{in,fix})_{k\geq 0}$ which is the constant sequence and $u_2(k) = \big(T_{in,fix} + \Delta T, T_{in,fix}, \ldots\big)$ for user defined values of $T_{in,fix}$ and ΔT. Hence, using the method described in Section 3 can be applied and leads to approximate values of the system coefficients

$$A\big(\dot{m}_{fix}\big) = A - c_p \cdot B \cdot \dot{m}_{fix}, \quad B\big(\dot{m}_{fix}\big) = c_p \cdot B \cdot \dot{m}_{fix}. \quad (26)$$

From these, the values for A and B can easily be determined. From the given references $y_1(k)$ or $y_2(k)$ one can then determine the disturbance $d(k)$. Finally, (21) can be included as an additional equation in the optimization constraints to describe the temperature dynamics of the BTES.

https://doi.org/10.52202/077185-0157

In the previous considerations, we assumed that the temperature dynamic of the BTES can be described by a single temperature T_{BT}. Due to the rather large BTES volume, the modeling equation (21) can be viewed as an average temperature which might lead to imprecisions. A more accurate modeling is provided by finite element methods, where the BTES and ground volume is divided into several user-defined sub-volumes of different temperatures. Hence it is expected that also the number of states of the identified system will increase, as the number of considered volumes increases.

Therefore, we describe in following the identification of the BTES temperature in this more general setting. Motivated by (21), we consider the following bilinear system class

$$\begin{aligned} x(k+1) &= (A_0 + m(k)A_1)x(k) + (B_0 + m(k)B_1)u(k) + d(k), \\ y(k) &= (C_0 + m(k)C_1)x(k) + (D_0 + m(k)D_1)u(k) \end{aligned} \tag{27}$$

for matrices $A_i \in \mathbb{R}^{\rho\times\rho}, B_i \in \mathbb{R}^{\rho}, C_i^\top \in \mathbb{R}^{\rho}, D_i \in \mathbb{R}^{\rho\times\rho},\ i = 0{,}1$. Hence, (27) for two fixed mass flows $\dot{m}_1$ and $\dot{m}_2$ is linear and we can identify the LTIs $(A_{m1}, B_{m1}, C_{m1}, D_{m1})$ and $(A_{m2}, B_{m2}, C_{m2}, D_{m2})$. Therefore, the system matrices can be obtained in the following way

$$A_1 = (m_2 - m_1)^{-1} \cdot (A_{m2} - A_{m1})\,, \qquad A_0 = A_{m2} - m_2 A_1, \tag{28}$$

and analogously for B_0, B_1, C_0, C_1, D_0 and D_1. In a second step, we assume now a constant disturbance $d = d(k)$ with the aim to identify values for d and the initial value $x(0)$ that fit to the given data sets. This can be achieved by applying a least squares fitting of the computed $y(k)$ using the determined system matrices with the given reference signals.

5 CASE STUDY OF ENERGY OPERATIONAL OPTIMIZATION FOR A BTES SYSTEM

In this section, we consider the heating network shown in Figure 1 and aim for operating the system at minimum electricity costs with respect to the constraints listed in Section 2. Here we optimize over one year, starting on the first day in January with a resolution of one hour for each time step. This leads to $N = 8760$ time steps using the following objective function

$$f\left(P_{hp}, P_{pk}\right) = \sum_{i=1}^{N} \nu_{pk}(i)P_{pk}(i) + \nu_{hp}(i)P_{hp}(i), \tag{29}$$

where ν_{pk} and ν_{hp} are the electricity costs to run the electric heater and the heat pump, respectively. For simplicity, we restrict ourselves in the case study to $\nu_{hp}(i) = 1$ for all $i = 1, \dots, N$. However, within the flexibility of a heating network, variable electricity prices are an important aspect to further reduce the costs and will be considered in future work.

The system identification is applied to simulation data generated from the simplified model (21), where the system parameters are fixed but assumed to be unknown. In the simulation, we consider a fixed mass flow $\dot{m}_{fix} = 20$ and set $T_{in,fix} = 30$, $\Delta T = 30$, yielding the input sequences $\mathrm{u}_1(1) = 60$, $\mathrm{u}_1(k) = 30, \mathrm{k} \geq 2$, and $\mathrm{u}_2(1) = 30$, $\mathrm{u}_2(k) = 30, \mathrm{k} \geq 2$ for the simulation setup. The identified system (11) was of order $n = 1$ and we determined its system matrices in (22) as $A = 0.99997961$ and $B = 1.1136 \cdot 10^{-8}$ with constant $d = 2.4355 \cdot 10^{-4}$. For the case study, we consider the parameters mentioned in Section 2 and the storage volume $V_{stts} = 1000\ m^3$. The considered heat demand $\dot{Q}_{dem}(k)$ is taken from rescaled data of a medium sized real district heating network and we use a site specific solar thermal heat flow $\dot{Q}_{sol}(k)$.

https://doi.org/10.52202/077185-0157

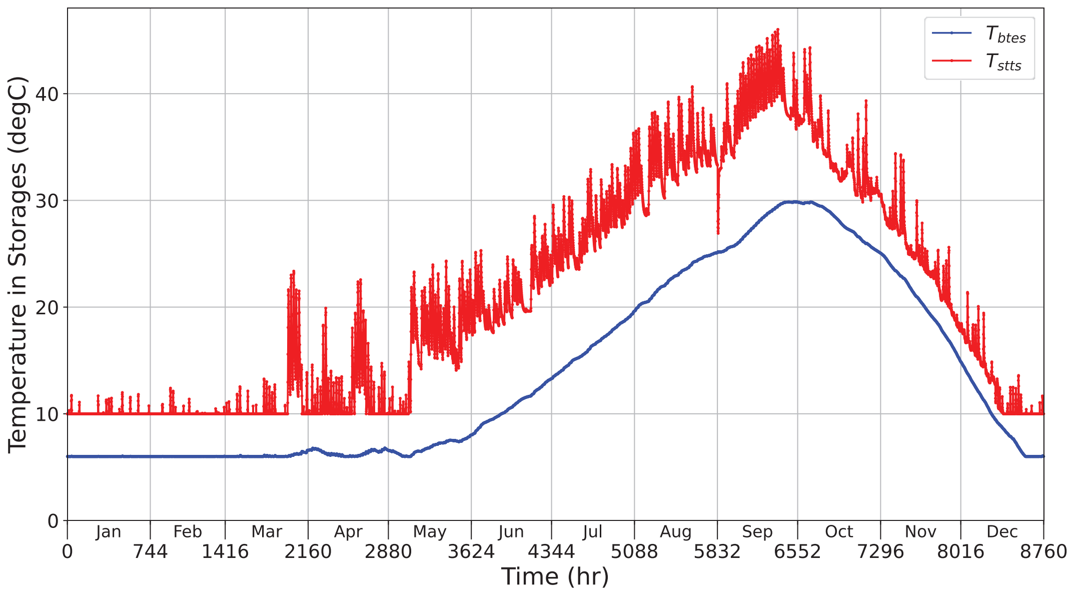

Figure 2: The storage temperatures in the STTS (red) and the BTES (blue) during the optimal operation which minimizes the used electrical power**.**

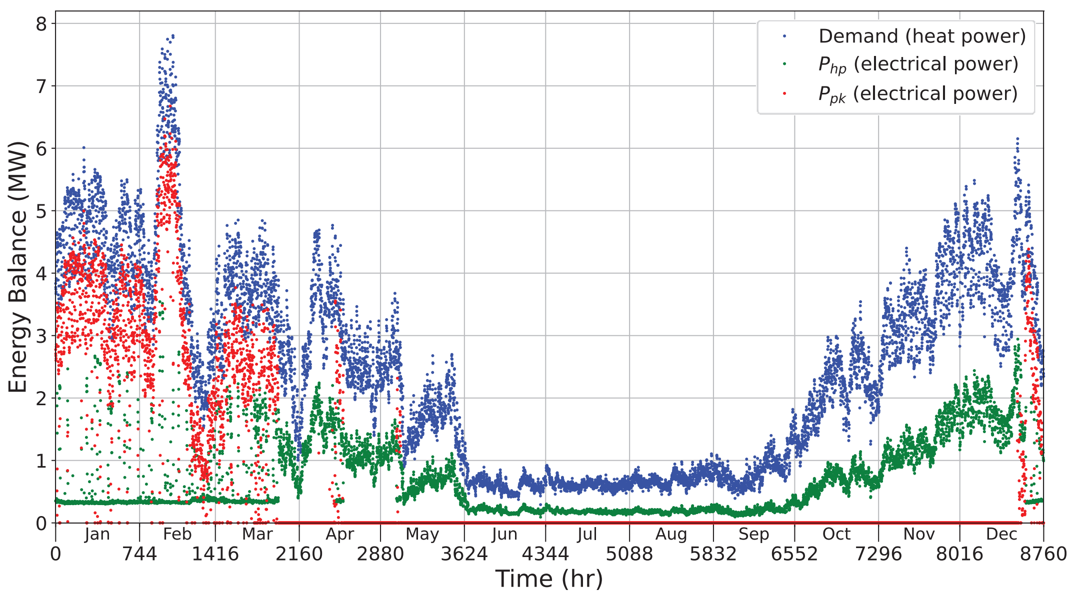

Figure 3: The annual heat demand (blue) is covered by the heat provided by the heat pump (green) and the peak load unit (red).

For the optimization, we used the Python optimization toolbox Pyomo with the solver IPOPT. The optimized storage temperatures in the STTS and BTES are shown in Figure 2. We observe high daily temperature fluctuations in the STTS and rather slow dynamics within the BTES. Also, the temperature levels are different. In the optimization, we set the lowest possible BTES temperature at 6 °C, which is also assumed to be the initial temperature of the BTES. This BTES temperature is almost maintained during January until beginning of May. During the summer, the BTES is charged and the temperature stays below 30 °C such that the storage could e.g. be used for cooling a data center throughout the year. Furthermore, the BTES is discharged at beginning of October when the heating period starts.

https://doi.org/10.52202/077185-0157

Figure 3 shows the heat demand covered by the heat pump and the peak load unit. Here we used a rescaled typical heat profile with high demands during the beginning and the end of the year and a comparably small demand in the middle of the year. We observe a rather high usage of the peak load unit during January until April, which is due to the fact that the BTES is not charged yet. Once the storage is charged the demand can be covered from October until mid of December only by using the heat pump.

6 CONCLUSION AND DISCUSSION

In this paper, we presented a dynamic model for a heat supply system, which incorporates the mass flows and temperatures. We used a method to obtain a control-oriented surrogate model from simulation data that can be incorporated easily within a dynamic optimization model aimed at minimizing the operating costs of a heating network by adjusting the electrical power used. The results were illustrated in a small numerical case study for a heat supply system that contains a BTES system.

Although the current method is promising, it also has its limitations. These limitations are addressed in the following discussion.

Regarding the modeling of the heat supply system, we do not include pipe models, since the pipe lengths on the production side are rather short. However, for district heating networks, the flow speed of water of 1-3 m/s is rather slow compared to the network length of several hundred meters up to a few kilometers. This introduces severe time delay effects on the heat dynamics between producers and consumers which need to be considered in the control of the system as well. Also, to further minimize exergy losses, it might be necessary to separate the hydraulics of a higher and a lower temperature level, which might require the modeling of a second heat pump operating in a lower temperature range.

Currently, the validation of the data-based surrogate modeling method relies on simulation data, especially simulations generated by the model (18) with unknown parameters, rather than FEM simulation data. To close this gap in validation, future efforts should prioritize the validation of the method using FEM simulation data. In addition, the choice of identification method should be considered and nonlinear system identification methods will be investigated to improve the robustness of the overall approach.

Regarding the particular demonstration site in Bochum, we plan to create digital FEM models of the Mine storage (MTES) using the Spring software system. Once the model is ready, the methodology presented here will be applied to generate the data-based surrogate models for the optimization. Based on the optimization, we will identify scenarios that are economically attractive for underground storage systems. Due to the rather fast computation of the optimal solution, it is possible to include an outer loop for design and sizing optimization of the heat supply system.

Regarding the optimization, we assume a perfect forecast. Since future data are not given for real systems, it is planned to apply a model predictive control, which incorporates a weather forecast for the next few days only and which might incorporate uncertainties. On the other hand, also the optimization horizon needs to be extended to several years to evaluate the performance of the storage.

ACKNOWLEDGEMENT

The authors gratefully acknowledge the funding within the PUSH-IT project by the European Union's Horizon Europe research and innovation programme under grant agreement No 101096566. Views and opinions expressed are however those of the authors only and do not necessarily reflect those of the European Union. Neither the European Union nor CINEA can be held responsible for them.

https://doi.org/10.52202/077185-0157

REFERENCES

Abdur Rehman, O., Palomba, V., Frazzica, A. and Cabeza, L.F., 2021, Enabling Technologies for Sector Coupling: A Review on the Role of Heat Pumps and Thermal Energy Storage, *Energies*, Vol. 14 No. 24, p. 8195.

Arpagaus, C., Bless, F., Uhlmann, M., Schiffmann, J. and Bertsch, S.S., 2018, High temperature heat pumps: Market overview, state of the art, research status, refrigerants, and application potentials, *Energy*, Vol. 152, pp. 985–1010.

Bynum, M.L., Hackebeil, G.A., Hart, W.E., Laird, C.D., Nicholson, B.L., Siirola, J.D., Watson, J.-P. and Woodruff, D.L., 2021, *Pyomo — Optimization Modeling in Python*, Vol. 67, 3rd ed. 2021, Springer International Publishing, Cham.

Danish Energy Agency, 2023, Technology CataloguesTechnology Data for Energy Storage, available at: https://ens.dk/en/our-services/projections-and-models/technology-data/technology-data-energy-storage (accessed 1 March 2024).

De Schutter, B., 2000, Minimal state-space realization in linear system theory: an overview, *Journal of Computational and Applied Mathematics*, Vol. 121 1-2, pp. 331–354.

European Union, 2020, *Long-term low greenhouse gas emission development strategy of the European Union and its Member States*.

Eurostat, 2022, *Share of energy from renewable sources*, Eurostat.

Fiorentini, M. and Baldini, L., 2021, Control-oriented modelling and operational optimization of a borehole thermal energy storage, *Applied Thermal Engineering*, Vol. 199, p. 117518.

Fiorentini, M., Heer, P. and Baldini, L., 2023, Design optimization of a district heating and cooling system with a borehole seasonal thermal energy storage, *Energy*, Vol. 262, p. 125464.

Hart, W.E., Watson, J.-P. and Woodruff, D.L., 2011, Pyomo: modeling and solving mathematical programs in Python, *Mathematical Programming Computation*, Vol. 3 No. 3, pp. 219–260.

Machado, J.E., Ferguson, J., Cucuzzella, M. and Scherpen, J.M.A., 2022, *Decentralized temperature and storage volume control in multi-producer district heating, IEEE Control Systems Letters,* Vol. 7, pp. 413-418.

Münnich, P., Metz, J., Hauser, P., Kohn, A. and Mühlpointner, T., 2022, *Power-2-Heat: Erdgaseinsparung und Klimaschutz in der Industrie*.

Petrecca, G., 1993, *Industrial Energy Management: Principles and Applications*, Springer US, Boston, MA.

Saloux, E. and Candanedo, J.A., 2019, Control-oriented model of a solar community with seasonal thermal energy storage: development, calibration and validation, *Journal of Building Performance Simulation*, Vol. 12 No. 5, pp. 523–545.

Verhelst, C. and Helsen, L., 2011, Low-order state space models for borehole heat exchangers, *HVAC&R Research No.* 17, pp. 928–947.

Victoria, M., Zhu, K., Brown, T., Andresen, G.B. and Greiner, M., 2019, The role of storage technologies throughout the decarbonisation of the sector-coupled European energy system, *Energy Conversion and Management*, Vol. 201, p. 111977.

VITO NV, 2023, Use Cases | Stormcontroller, available at: https://stormcontroller.eu/en/use-cases (accessed 11 October 2023).

https://doi.org/10.52202/077185-0157